Oral Oncology 142 (2023) 106433

Contents lists available at ScienceDirect

Oral Oncology

journal homepage: www.elsevier.com/locate/oraloncology

EpEX, the soluble extracellular domain of EpCAM, resists cetuximab treatment of EGFR-high head and neck squamous cell carcinoma

Koki Umemori [a], Kisho Ono [a,*], Takanori Eguchi [b], Hotaka Kawai [c], Tomoya Nakamura [a], Tatsuo Ogawa [a], Kunihiro Yoshida [a], Hideka Kanemoto [a], Kohei Sato [a], Kyoichi Obata [a], Shoji Ryumon [a], Hirokazu Yutori [a], Naoki Katase [d], Tatsuo Okui [e], Hitoshi Nagatsuka [c], Soichiro Ibaragi [a]

[a] Department of Oral and Maxillofacial Surgery, Faculty of Medicine, Dentistry and Pharmaceutical Sciences, Okayama University, Okayama 700-8525, Japan
[b] Department of Dental Pharmacology, Faculty of Medicine, Dentistry and Pharmaceutical Sciences, Okayama University, Okayama 700-8525, Japan
[c] Department of Oral Pathology and Medicine, Faculty of Medicine, Dentistry and Pharmaceutical Sciences, Okayama University, Okayama 700-8525, Japan
[d] Department of Oral Pathology, Graduate School of Biomedical Sciences, Nagasaki University, Nagasaki 852-8588, Japan
[e] Department of Oral and Maxillofacial Surgery, Shimane University Faculty of Medicine, Izumo, Shimane 693-8501, Japan

ARTICLE INFO

Keywords:
Cetuximab
epithelial cell adhesion molecule (EpCAM)
EpEX
EpICD
epidermal growth factor receptor (EGFR)
Drug resistance
Head and neck squamous cell carcinoma (HNSC)

ABSTRACT

Objectives: Cetuximab (Cmab) is a molecularly targeted monoclonal antibody drug for head and neck squamous cell carcinoma (HNSC), although cetuximab resistance is a serious challenge. Epithelial cell adhesion molecule (EpCAM) is an established marker for many epithelial tumors, while the soluble EpCAM extracellular domain (EpEX) functions as a ligand for epidermal growth factor receptor (EGFR). We investigated the expression of EpCAM in HNSC, its involvement in Cmab action, and the mechanism by which soluble EpEX activated EGFR and played key roles in Cmab resistance.

Materials and methods: We first examined *EPCAM* expression in HNSCs and its clinical significance by searching gene expression array databases. We then examined the effects of soluble EpEX and Cmab on intracellular signaling and Cmab efficacy in HNSC cell lines (HSC-3 and SAS).

Results: EPCAM expression was found to be enhanced in HNSC tumor tissues compared to normal tissues, and the enhancement was correlated with stage progression and prognosis. Soluble EpEX activated the EGFR-ERK signaling pathway and nuclear translocation of EpCAM intracellular domains (EpICDs) in HNSC cells. EpEX resisted the antitumor effect of Cmab in an EGFR expression-dependent manner.

Conclusion: Soluble EpEX activates EGFR to increase Cmab resistance in HNSC cells. The EpEX-activated Cmab resistance in HNSC is potentially mediated by the EGFR-ERK signaling pathway and the EpCAM cleavage-induced nuclear translocation of EpICD. High expression and cleavage of EpCAM are potential biomarkers for predicting the clinical efficacy and resistance to Cmab.

Introduction

The molecularly targeted drug cetuximab (Cmab) is an anti-epidermal growth factor receptor (EGFR) IgG1 monoclonal antibody currently used for the treatment of locally advanced or recurrent/metastatic head and neck cancer (HNC) [1–3] and Ras-wildtype metastatic colorectal cancer. Direct binding of Cmab to EGFR can prevent cancer growth by inhibiting the ligand interaction, dimerization, and phosphorylation of EGFR and the downstream Ras-Raf-MEK-ERK signaling pathway [1,4]. In head and neck squamous cell carcinoma (HNSC), Cmab monotherapy was previously reported effective in 13% of patients with recurrent or metastatic HNSC and improved overall survival when combined with radiation therapy or chemotherapy [5]. On the other hand, serious side effects, low response rates, and residual tumors after

Abbreviations: Cmab, cetuximab; CSC, cancer stem cell; EGF, epidermal growth factor; EGFR, epidermal growth factor receptor; EpCAM, epithelial cell adhesion molecule; EpEX, extracellular domain of EpCAM; EpICD, intracellular domain of EpCAM; FL, full-length; HNC, head and neck cancer; HNSC, head and neck squamous cell carcinoma.

* Corresponding author.
E-mail address: de20012@s.okayama-u.ac.jp (K. Ono).

https://doi.org/10.1016/j.oraloncology.2023.106433
Received 13 March 2023; Received in revised form 14 April 2023; Accepted 15 May 2023
Available online 24 May 2023

treatment remain problems for EGFR inhibitors, including Cmab [6]. To solve these problems, it is necessary to understand the mechanism of Cmab resistance and to take countermeasures against it. Two major mechanisms of Cmab resistance in tumors have been identified: (i) the constant increase in proliferative signaling levels associated with changes in EGFR-ligand or molecules mediating the EGFR signaling pathway, such as Ras [7], and (ii) the use of other surface receptors, such as ERBB2 and MET, in the tumor cell proliferative system [8–10]. Mutations in KRAS and other downstream factors of EGFR are rare in HNC. However, there is no useful biomarker to predict and diagnose Cmab resistance. In the present study, we hypothesized that epithelial cell adhesion molecule (EpCAM) is involved in the EGFR signaling and Cmab resistance in HNSC.

EpCAM is a type I transmembrane (TM) glycoprotein composed of 314 amino acids (aa) that resides on the cell membrane surface and influences cellular functions toward tumor progressions, such as cell adhesion, cell proliferation, and cancer stemness [11–13]. EpCAM is highly expressed in epithelial cancers and is a potential diagnostic and prognostic marker for the progression of cancers of epithelial origin, including HNSC [14]. The full-length (FL) EpCAM consists of an N-terminal signal peptide, an extracellular domain (EpEX: 242 aa), a *trans*-membrane domain (23 aa), and a C-terminal intracellular domain (EpICD: 26 aa) [13,15]. EpEX contains epidermal growth factor (EGF)-like domain I and II (also known as N-domain: 40 aa), thyroglobulin type-1A-repeat-like (TY) domain (75 aa), and cysteine-free domain (127 aa), while EpICD has two binding sites for alpha-actin cytoskeleton [12,13,15]. In addition to its role in cell adhesion, EpCAM can function as an intracellular and nuclear signaling molecule. When cleaved at the plasma membrane, EpICD can bind with β-catenin, and the molecular complex regulates the transcription of target genes [15]. Nuclear EpICD is expected to be useful as a biomarker for cancer metastasis and prognosis [15–17]. Moreover, a cleaved soluble form of EpEX can bind to EGFR as a ligand and activate downstream cascades to enhance tumor cell proliferation and progression [15,18–20].

However, the role of EpCAM in Cmab resistance has yet to be clarified. To clarify EpCAM expression and its involvement in Cmab action and resistance in HNSC, we examined the mechanism by which soluble EpEX altered both EGFR signaling and the cellular EpCAM status involved in Cmab resistance.

Methods

Data acquisition

RNA sequence data of HNSC patients (TCGA-HNSC), which were taken from 44 normal tissue samples and 504 tumor tissue samples, were downloaded from the TCGA portal (https://portal.gdc.cancer.gov/) and divided into "*EPCAM*-high" and "*EPCAM*-low" groups according to the median transcript per million (TPM) value of *EPCAM* expression (Median = 45.3361). Clinical data corresponding to the TCGA-HNSC cohort were downloaded from cBioPortal (https://www.cbioportal.org/).

EPCAM expression in the TCGA-HNSC cohort

The differential expression of *EPCAM* between normal tissue samples (N = 44) and tumor tissue samples (N = 504) was analyzed in boxplot, using R v4.2.1 [21] (The R Foundation for Statistical Computing, Vienna, Austria; https://www.r-project.org/). We also compared *EPCAM* expression between the paired normal tissue and tumor tissue samples (N = 43). The TPM + 1 values were log2-transformed and then compared.

Expression analysis of EPCAM in HNSC cases

To compare *EPCAM* gene expression levels by HNSC stages I to IV, we used the OncoDB data set (https://oncodb.org/index.html) [22].

Correlation between EPCAM expression and prognosis

Kaplan-Meier plotting from RNA-seq data was performed using KM plotter [23,24]. We analyzed the overall survival of HNSC patients (n = 500) with auto-select best cutoff.

The correlation between clinical data and EPCAM expression

Pearson's Chi-square test and Fisher's exact test were used to evaluate the correlation between the *EPCAM* expression and clinicopathological characteristics. Cox proportional hazard model was used for multivariate analysis. All analyses were conducted using R v4.2.1.

Tissue microarray

The expression of EpCAM was analyzed in head and neck cancer and in a normal tissue microarray (OR601c; US Biomax). Antigens were activated by autoclaving in a citric acid solution. For immunohistochemistry, specimens were incubated with anti-EpCAM antibody (1:500) overnight at 4 °C) and then treated with avidin–biotin complex (1:100, VECTASTAIN ABC kit; Vector Laboratories, CA) for 60 min. The immunoreaction was visualized using DAB substrate-chromogen solution (SK-4100 DAB substrate kit; Vector Laboratories).

Cell culture

SAS and HSC-3 were obtained from JCRB Cell Bank and cultured in DMEM containing 10% FBS in a humidified incubator at 37 °C and 5% CO_2 as previously described [25].

Three-dimensional (3D) spheroid culture

The 3D spheroid culture was performed as previously described [25–28]. Briefly, 1.0×10^5 cells were seeded into each well of a 96-well ultra-low attachment (ULA) plate (#7007; Corning, NY). Spheroid images were captured using a bright-field microscope (IX81; Olympus, Tokyo).

Reagents

Antibodies against EGFR (ab32562), EpICD (ab32392), and KDM1/LSD1 (ab129195) and HRP-conjugated anti-β-actin antibody (ab49900) were purchased from Abcam (Cambridge, MA). Antibodies against EpCAM (VU1D9), p-EGFR (D7A5), E-cadherin (24E10), p44/42 MAPK (L34F12), and p-p42/44 MAPK (T202/Y204) were purchased from Cell Signaling Technology (Danvers, MA).

Recombinant human (rh) EGF (585506) and CD326/EpCAM EpEx (777306: Gln24–Lys265, Accession #P16422) were obtained from BioLegend (San Diego, CA) and resolved in PBS.

Cetuximab (Erbitux® Injection) was obtained from Merck Serono (Tokyo).

Treatment with recombinant proteins and antibodies

EGF or EpEX was used at a final concentration of 50 nM. The effect of EpEX was determined in transitional time (0, 3, 6, 12, 24, or 48 h). The

effect of Cmab was determined 24 or 48 h after the addition. EpEX and Cmab were added to the formed spheroids 24 h after cell seeding in the ULA plate [25]. Each material was re-added when the media were changed every three days.

Cell viability

Cmab and EpEX were added to cells at final concentrations of 100 nM and 40 nM, respectively, 24 h after cell seeding. Cells were detached or disassembled using Trypsin/EDTA. The number of cells was counted using a Countess® Automated Cell Counter (Thermo Fisher Scientific).

Western blotting (WB)

The whole cell lysate (WCL) was prepared as previously described [29,30]. Briefly, cells cultured in a 10-cm dish were lysed in 200 μl/dish of RIPA buffer (1% NP-40, 0.1% SDS, 0.5% deoxycholate, and EDTA-free protease inhibitor cocktail in PBS) and collected by using cell scrapers. Cells were further lysed using a 25-gauge syringe for 10 S and then incubated for 30 min on ice. Spheroids were treated with ultrasonic crushing. Protein concentrations were analyzed using a BCA protein assay (Thermo Fisher Scientific). Equal amounts of WCL were subjected to SDS-PAGE, then transferred to a PVDF membrane using a semi-dry method. Membranes were blocked in 5% skim milk in Tris-buffered saline containing 0.05% Tween-20 for 60 min, incubated with primary antibodies, and then incubated with HRP-conjugated secondary antibodies. Blots were visualized using Clarity ECL substrate and a ChemiDoc MP system (Bio-Rad, Hercules, CA).

Nuclear and cytoplasmic extracts

Cells were collected 3, 6, 12, and 24 h after EpEX stimulation and dissolved in PBS. We centrifuged lysates, removed the supernatant, and added Nuclear and Cytoplasmic Extraction Reagents (#78833; Thermo Fisher Scientific) to the cell pellet. Each fraction was then extracted.

Immunocytochemistry

Immunocytochemistry was performed as previously described [25,31]. Cells were treated with rhEGF or EpEX for 6 h, fixed with 4% paraformaldehyde (PFA) for 20 min, and permeabilized with 0.1% Triton-X100 for 10 min. Fixed cells were treated with methanol containing 0.3% H_2O_2 and blocked within 3% BSA in PBS containing 0.1% Tween-20 for 30 min at RT. Slides were incubated with anti-EpCAM (dilution 1:100) or anti-EGFR antibodies (dilution 1:100) overnight at 4 °C and with anti-rabbit IgG AlexaFluor488 for 60 min and DAPI. Fluorescence images were taken using a BZ-X700 microscope (Keyence, Osaka, Japan). Confocal images were taken using a Zeiss LSM780 microscope with a 40 × objective lens at Central Research Laboratory, Okayama University Medical School.

Immunohistochemistry of spheroid sections

Spheroid sections were prepared as previously described [11,25–27]. Briefly, spheroids were washed with PBS, fixed in 4% PFA for 30 min, and embedded in paraffin. Spheroid sections (3 μm thickness) were deparaffinized and hydrated through xylenes and a graded alcohol series. Sections were treated with proteinase K solution for 5 min and blocking solution (Dako, Carpenteria, CA) for 30 min at RT. Immunohistochemistry was performed as previously described [25] using anti-EpCAM (dilution 1:800) and anti-EGFR (dilution 1:100) antibodies.

Hypoxia detection assay of spheroids

Hypoxia detection assay was performed as previously described [11,26,32]. Briefly, hypoxia conditions of spheroids were measured using a hypoxia probe solution (LOX-1; MBL, Nagoya, Japan). Fluorescence images and intensities of spheroids were taken using a BZ-X700 microscope (Keyence).

Statistical analysis

Statistical significance was calculated using Microsoft Excel and EZR software (jichi.ac.jp/saitama-sct/SaitamaHP.files/statmedEN.html). Differences between two data sets were examined with a Mann-Whitney *U* test, and more than three sets of data were examined with a Kruskal-Wallis test; values of $p < 0.05$ were considered to indicate statistical significance. Data were expressed as means ± S.D. unless otherwise specified.

Results

High expression of EPCAM is a prognostic marker for a poor prognosis of HNSC

To examine the potential association between *EPCAM* expression and prognosis in HNSC, we used the public TCGA database. We found that *EPCAM* was more highly expressed in tumor tissues than in normal tissues in the head and neck regions (Fig. 1A). The same trend was also observed for each tumor tissue versus normal tissue within the same HNSC case (Fig. 1B). In addition, *EPCAM* expression was enhanced as the tumor stage progressed (Fig. 1C), and overall survival was significantly lower in the high *EPCAM* expression group compared to the low *EPCAM* expression group in HNSC (Fig.1D). Moreover, the TCGA database analysis showed that *EPCAM* expression was significantly correlated with the degree of differentiation, angiolymphatic invasion, perineural invasion, extracapsular spread, tumor mutational burden, and HPV status (ISH) (Table 1). We further showed by chi-square test that there were significant differences in *EPCAM* expression by subsite, and by residual analysis that *EPCAM* expression was significantly higher in the pharynx and tonsils, but significantly lower in the tongue (Table S1). Immunohistochemistry demonstrated that EpCAM at protein expression levels in tumor tissues of HNSCs appeared to be more positively stained compared to normal tissues (Fig. 1E). Interestingly, EpCAM tended to be stained in the cell membrane of tumor cells in the majority of cases, although some showed nuclear staining (Fig. 1E).

These results suggested that EpCAM expression in HNSC might be a useful biomarker for predicting poor prognosis.

Sensitivity to cetuximab depends on the EGFR expression level in HNSC cells

To examine whether differential expression levels of EGFR or EpCAM between HSC-3 and SAS cells were associated with the Cmab sensitivity, we compared the relative expression levels of EGFR and EpCAM in these cell lines. We have previously examined the biological background of the HNSC cell lines used in detail [25]. EGFR expression was significantly higher in HSC-3 than in SAS cells, consistent with a recent report [25] (Fig. 2A,B). In contrast, EpCAM expression was significantly higher in SAS than in HSC-3 cells (Fig. 2A,B). Cmab treatment significantly reduced the viabilities of both cell lines, but the reduction was more significant in the subset of HSC-3 cells that had predominant EGFR expression (Fig. 2C,D). In the following experiments, we utilized these cell lines with different basal expressions of EGFR and Cmab sensitivities

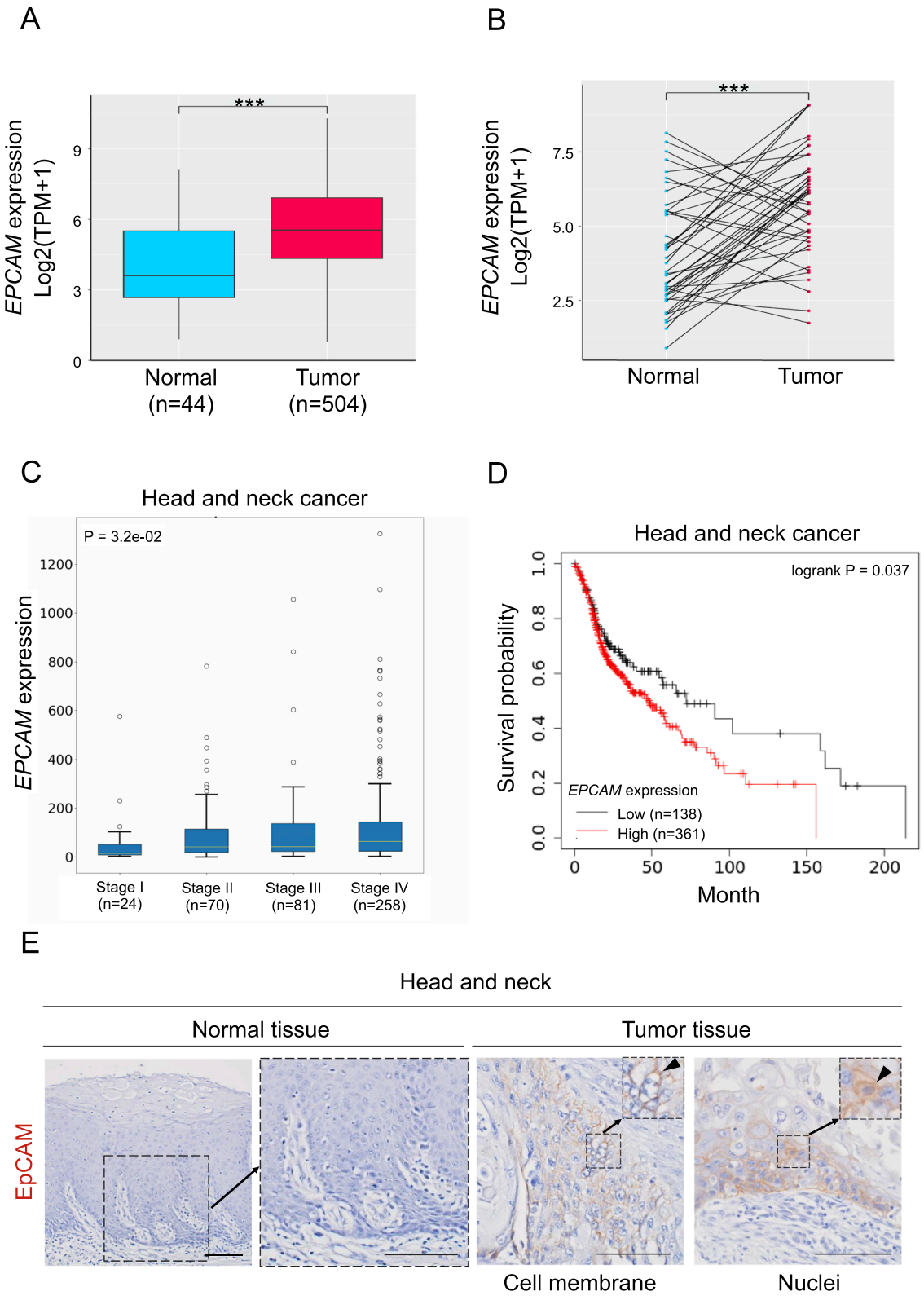

Figure 1. Prognostic value of *EPCAM* gene expression in HNSC cases. gene expression in HNSC cases. (A,B) *EPCAM* gene expression in normal vs. tumor tissues in the head and neck region was analyzed using the TCGA database. (A) Box-and-whisker plots, (B) dot-and-line plots. ***p < 0.005. (C) Box-and-whisker plots for *EPCAM* gene expression by HNSC stages I to IV were retrieved from the OncoDB. ANOVA analysis was used. (D) Kaplan-Meier survival analysis for *EPCAM* gene expression. (E) Immunohistochemistry of EpCAM protein in normal and tumor tissues of the head and neck region retrieved from tissue microarray. Scale bars, 100 μm.

Table 1
Correlation between clinicopathological parameters and *EPCAM* expression.

		EPCAM expression (TPM)		
		Cut off = Median (45.3361)		
	Total N = 502	*EPCAM* High	*EPCAM* Low	p-value
		(N = 251)	(N = 251)	
Age				
≧60	N = 279	142	137	0.689
<60	N = 222	109	113	
Gender				
Male	N = 369	203	166	**1.82E-04**
Female	N = 133	48	85	
Race				
White	N = 428	217	211	0.477
Others*	N = 59	27	32	
Differentiation				
Well	N = 361	168	193	**0.021**
Moderate-poor	N = 121	71	50	
T stage				
T1-T2	N = 178	81	97	0.108
T3-T4	N = 309	164	145	
N stage				
N0	N = 240	114	126	0.144
N+	N = 240	130	110	
M-stage				
M0	N = 472	235	237	0.179
M1	N = 5	4	1	
TNM stage				
I-II	N = 115	44	71	**0.003**
III-IV	N = 373	201	172	
Surgical margin				
Positive	N = 106	51	55	0.734
Negative	N = 344	172	172	
Angiolymphatic invasion				
Positive	N = 120	77	43	**0.04**
Negative	N = 122	93	29	
Perineural invasion				
Positive	N = 165	68	97	**0.003**
Negative	N = 188	107	81	
Extracapsular spread				
Positive	N = 111	64	47	**0.02**
Negative	N = 237	105	132	
Prior malignancy				
Positive	N = 23	12	11	0.831
Negative	N = 479	239	240	
Tumor mutational burden				
TMB-H (≧10)	N = 66	43	23	**0.008**
TMB-H (<10)	N = 432	206	226	
HPV (ISH)				
Positive	N = 19	14	5	**0.040**
Negative	N = 64	30	34	
HPV (p16)				
Positive	N = 31	21	10	0.056
Negative	N = 72	34	38	

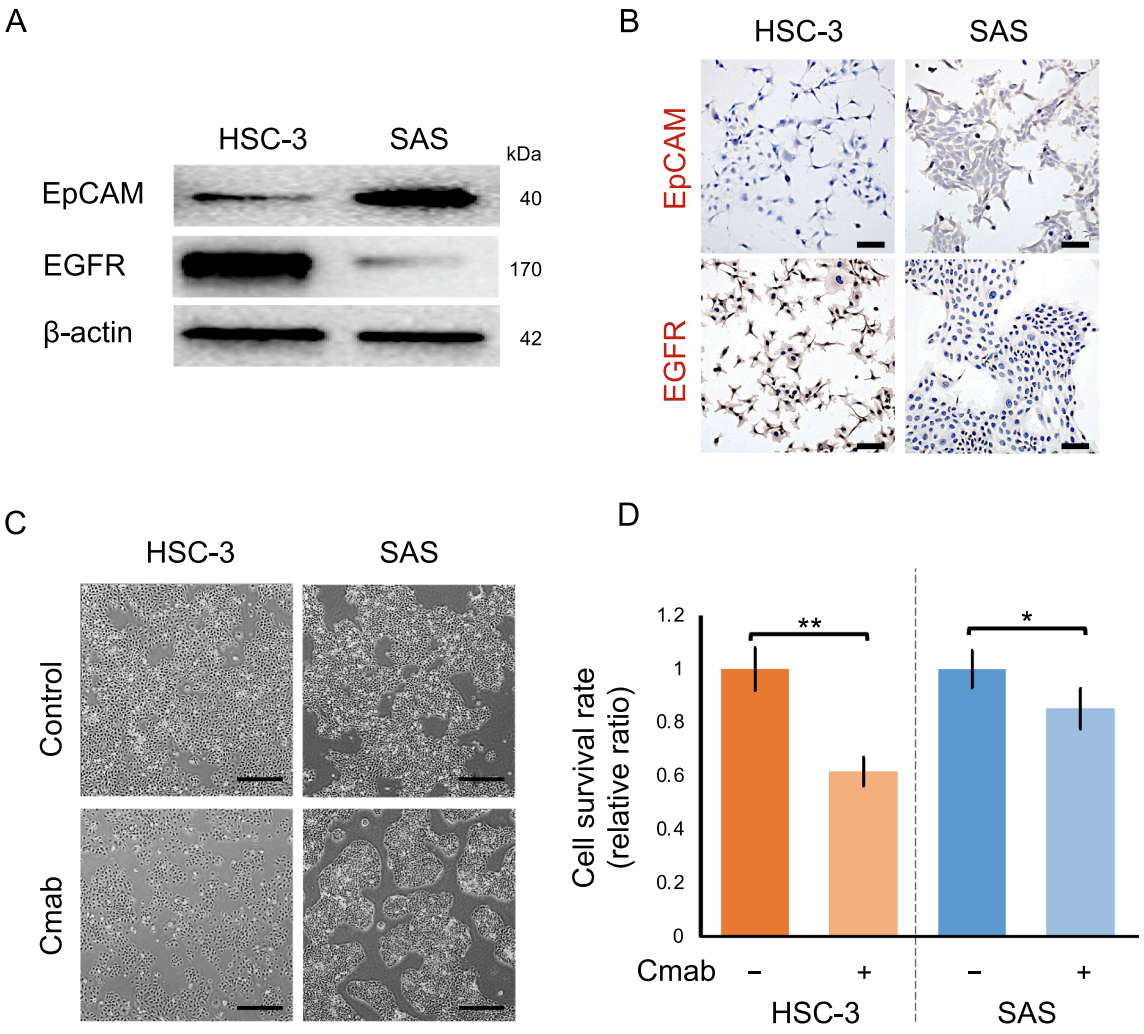

Figure 2. Differential EpCAM and EGFR expression levels in HSC-3 and SAS cells. (A) WB showing EpCAM and EGFR. β-actin was used as a loading control. (B) Immunocytochemistry for EpCAM and EGFR. Scale bars, 100 μm. (C) Representative images of monolayer-cultured cells with or without Cmab. Scale bars, 200 μm. (D) Cell survival rates with or without Cmab treatment for 24 h. n = 6. *p < 0.05, **p < 0.01 (Mann-Whitney *U* test).

in the following experiments.

EpEX enhances the EGFR-ERK signaling pathway and nuclear translocation of EpICD in HNSC cells

The EpEX domain contains EGF-like domains I and II, which can act as a ligand for EGFR (Fig. 3A) [12]. We examined the responses of two cell lines (HSC-3 and SAS) to the EGF and EpEX stimulations (Fig. 3A,B). The EGF stimulation increased the phosphorylation of EGFR and simultaneously reduced cellular FL-EpCAM in HSC-3 cells, whereas SAS did not respond to the EGF stimulation (Fig. 3C). Moreover, the EGF stimulation appeared to promote nuclear translocation of EpCAM, as estimated by the level of EpICD (Fig. S1).

The soluble EpEX enhanced the phosphorylation of EGFR and reduced cellular FL-EpCAM in HSC-3 cells (Fig. 3D) but not in SAS cells. And the trend occurred in a concentration-dependent manner for soluble EpEX (Fig. S2). To confirm the nuclear translocation of EpICD, we next separated the nuclear and cytoplasmic fractions and performed western blotting. The soluble EpEX stimulation promoted the nuclear translocation of EpICD and phospho-ERK in HSC-3 and SAS cells (Fig. 3E). Immunocytochemistry confirmed that the soluble EpEX stimulation promoted the nuclear translocation of EpICD (Fig. 3F). The phospho-ERK in nuclei increased 3 h after the EpEX stimulation, followed by EpICD nuclear translocation 6 h after the stimulation (Fig. S3).

These data suggested that EpEX as a ligand for EGFR enhanced the EGFR-ERK signaling pathway and the nuclear translocation of EpICD.

Soluble EpEX stimulation cancels the antitumor effects of cetuximab

We hypothesized that the soluble EpEX, containing EGF-like motifs, competes with Cmab, an anti-EGFR therapeutic antibody. Accordingly, we next examined the impact of EpEX on the Cmab treatment of HSC-3 and SAS cells. Treatment with Cmab alone significantly reduced the cell survival rates in HSC3 and SAS cells, whereas administration of soluble EpEX alone did not alter the survival rates. Incidentally, soluble EpEX also did not affect the cell proliferation of HNSC cell (Fig. S4). Of note, the cell survival rates were significantly greater by Cmab + EpEX treatment than by treatment with Cmab alone (Fig. 4A,B), suggesting that the soluble EpEX competed with Cmab and resisted the effects of Cmab.

We next asked whether the competition between EpEX and Cmab affected ERK phosphorylation. We found that treatment with Cmab alone markedly reduced the ERK phosphorylation level in HSC-3 cells, whereas Cmab + EpEX treatment recovered ERK phosphorylation to over the basal level in these cells (Fig. 4C). Such competition and stimulatory effects were found in HSC-3 cells, which expressed EGFR at high levels, but not in SAS cells, which barely expressed EGFR, as shown in Fig. 2.

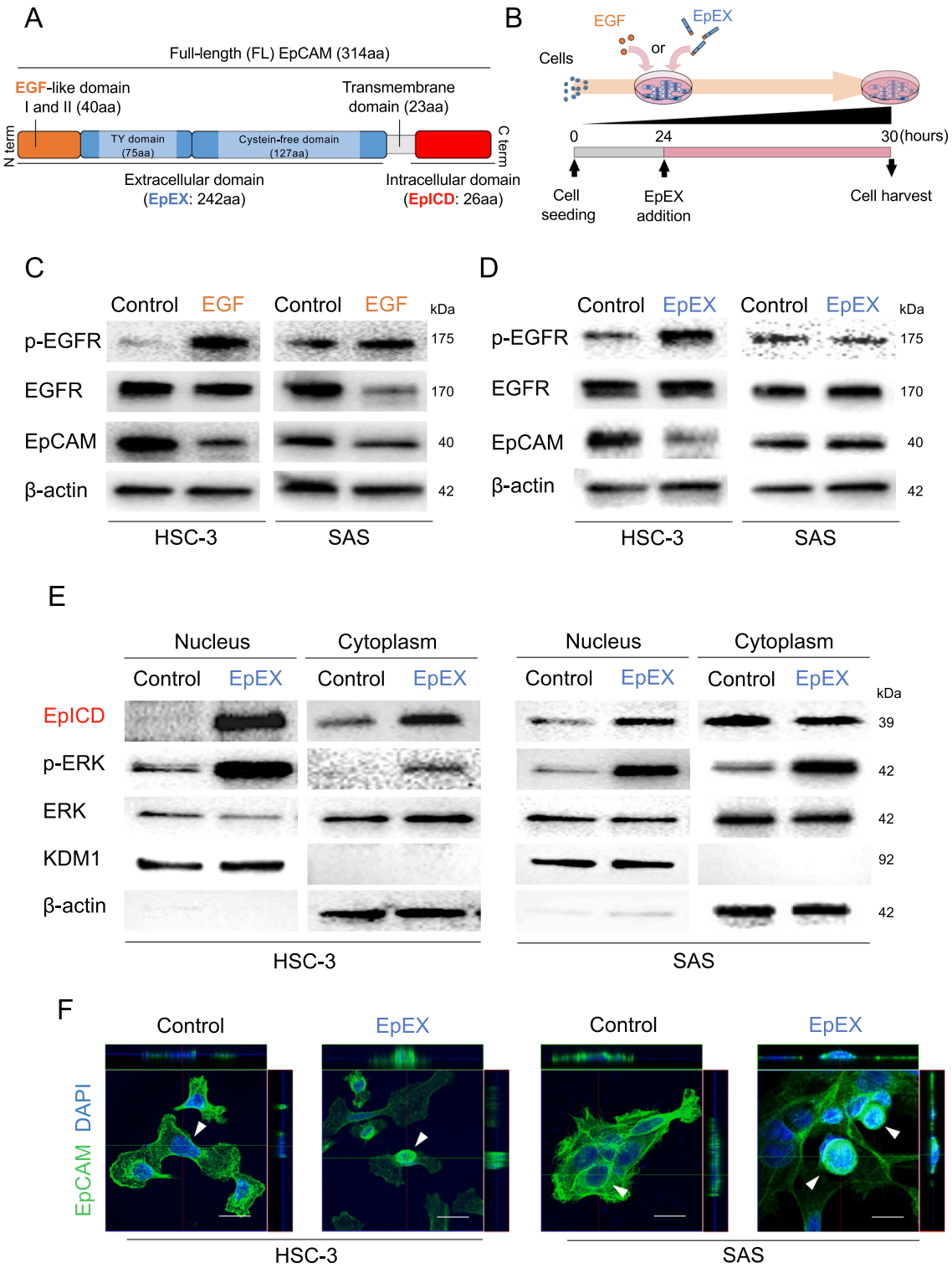

Figure 3. EpEX stimulation promotes nuclear translocation of EpICD via EGFR phosphorylation in HSC-3 and SAS cells. (A) Schematic of the structure of human EpCAM. The full-length EpCAM consists of an EpCAM extracellular domain (EpEX), a transmembrane domain, and an intracellular domain (EpICD). (B) Schematic diagram of the EGF or EpEX stimulation experiments. (C) WB showing p-EGFR, EGFR, and EpCAM with or without EGF stimulation. β-actin was used as a loading control. (D) WB showing p-EGFR, EGFR, and EpCAM with or without EpEX stimulation. β-actin was used as a loading control. (E) WB of EpICD, p-ERK, and ERK in nuclear and cytoplasmic fractions with or without EpEX stimulation. KDM1 was used as a nuclear marker. β-actin was used as a cytoplasmic marker. (F) Confocal laser scanning microscopy showing subcellular localization of EpCAM with or without EpEX stimulation. White arrowheads indicate the representative cell nuclei. Scale bars, 100 μm.

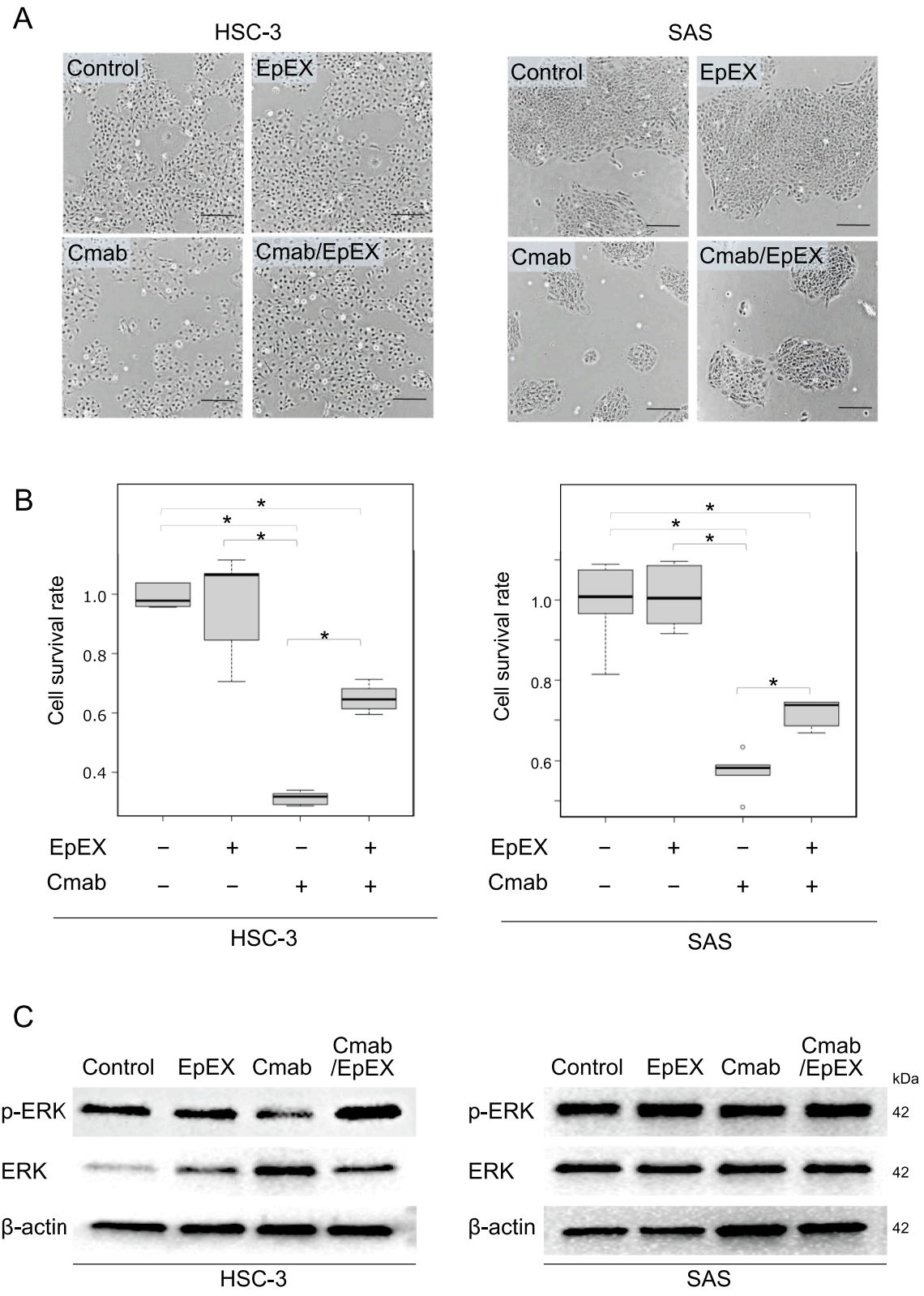

Figure 4. Effect of EpEX stimulation on the antitumor effect of Cmab on HNSC cells. HSC-3 and SAS cells were treated or non-treated with EpEX, Cmab or both EpEX/Cmab for 48 h. (A) Representative cell images of HSC-3 and SAS cells. Scale bars, 200 μm. (B) Cell survival rates. n = 6. *$p < 0.05$ (Kruskal-Wallis test). (C) WB of p-ERK and ERK. β-actin was used as a loading control.

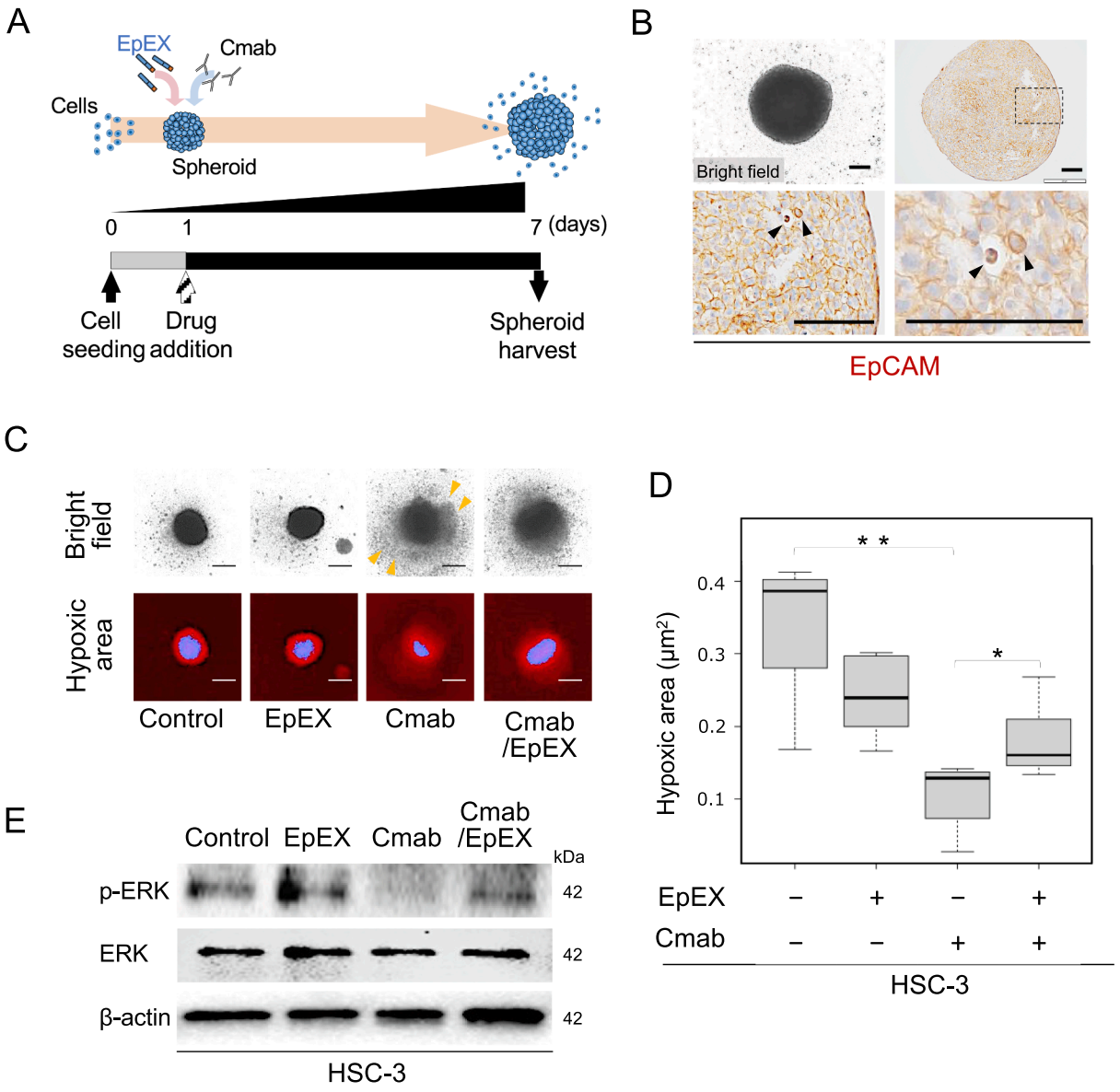

Figure 5. EpEX resists the antitumor effect of Cmab on HNSC spheroids. (A) Schemes of the spheroid culture of HSC-3 cells treated with Cmab and/or EpEX. (B) Immunohistochemistry showing EpCAM in spheroids. Arrowheads indicate nuclear localization of EpCAM. Scale bar, 100 μm. (C) Representative images of spheroids in bright fields and hypoxic areas. Yellow arrowheads indicate cells scattered by spheroid collapse. The blue areas indicate hypoxic areas over a defined cutoff value. The red areas indicate hypoxic areas below a defined cutoff value. Scale bar, 500 μm. (D) Box-whisker plots of hypoxic areas within spheroids. n = 10. *p < 0.05, **p < 0.01 (Kruskal-Wallis test). (E) WB showing p-ERK and ERK in HSC-3 spheroids. β-actin was used as a loading control. (For interpretation of the references to colour in this figure legend, the reader is referred to the web version of this article.)

These data suggested that the soluble EpEX competed against Cmab and stimulated the EGFR-ERK signaling pathway in EGFR-high HNSC.

The soluble EpEX abolishes the Cmab treatment in the HNSC spheroid model

We previously established 3D cultured spheroid/tumoroid models useful for cancer pharmacological research [25–28]. In the present study, therefore, we next asked whether the soluble EpEX would compete against Cmab and stimulate the ERK signaling pathway in a 3D culture model of HNSC cells (Fig. 5A). By immunostaining of HSC-3 spheroid sections, we found that EpCAM was mostly localized at intercellular adhesion sites, while the nuclear localization of EpCAM, supposed as estimated by the level of EpICD, was found in some cells (Fig. 5B). Cmab treatment caused the spheroid to collapse (Fig. 5C), but the soluble EpEX stimulation did not. Treatment with Cmab alone significantly reduced the hypoxic area of the spheroids and significantly reduced the number of spheroids that collapsed, whereas Cmab + EpEX treatment resulted in a larger hypoxia area of spheroids compared to treatment with Cmab alone (Fig. 5C,D). Furthermore, the inhibition of ERK phosphorylation by Cmab was also abolished by the simultaneous stimulation of EpEX in the HSC-3 spheroids (Fig. 5E).

These data suggested that the soluble EpEX contributed to the resistance of HNSC to Cmab by stimulating the EGFR-ERK signaling pathway (Fig. 6).

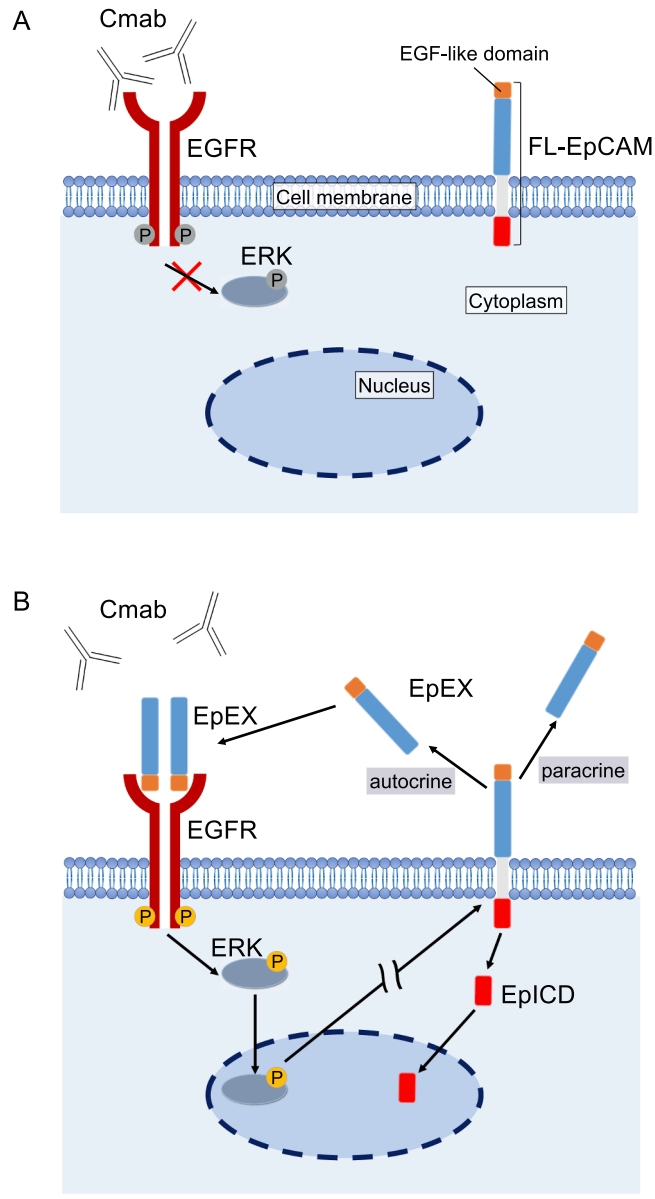

Figure 6. Schematic illustration of the mechanism of EpCAM-induced Cmab resistance via the EGFR pathway. (A) Cmab exerts its antitumor effects by directly binding to EGFR and inhibiting EGFR ligand interactions, dimerization, phosphorylation, and downstream EGFR-ERK signaling pathways. (B) EpEX, containing an EGF-like domain, binds to EGFR, exerts a competitive antagonistic effect on Cmab, and activates the EGFR-ERK signaling pathway. Subsequently, FL-EpCAM on the plasma membrane is cleaved, facilitating cytoplasmic and nuclear translocation of EpICD. These cellular events contribute to increased Cmab resistance in HNSC.

Discussion

Our study demonstrated that EpEX, the soluble extracellular domain of EpCAM, resists cetuximab treatment of EGFR-high HNSC (such as HSC-3 cells). We first showed that high expression of EpCAM is a useful prognostic marker for a poor prognosis of HNSC (Fig. 1). Among various HNSC, sensitivity to cetuximab may depend on the EGFR expression level in HNSC cells (Fig. 2). Of note, The soluble EpEX activated the EGFR-ERK signaling pathway and promoted nuclear translocation of EpICD in HNSC cells (Fig. 3). Moreover, soluble EpEX stimulation canceled the antitumor effects of cetuximab in mono-layer and 3D culture models of HNSC (Figs. 4, 5). These findings demonstrated that EpEX resisted cetuximab treatment of EGFR-high HNSC potentially via the nuclear translocation of EpICD and phosphorylated ERK.

Our study touched upon the mechanism by which soluble EpEX, a ligand of EGFR, resists Cmab therapy (Figs. 2–5). Cmab, a monoclonal antibody specific for the extracellular domain of EGFR, inhibits ligand binding and receptor phosphorylation, resulting in a strong growth inhibition effect in cells that grow in an EGFR pathway-dependent manner [33]. It has been shown that Cmab resistance is caused by direct changes in cell surface EGFR, such as cytoplasmic or nuclear localization of EGFR or dysregulation of EGFR internalization and degradation as by the epithelial-mesenchymal transition (EMT) of cancer cells [1–3,7]. Our previous study showed for the first time that HNSC cells exposed to Cmab were spared the antitumor effects by extracellular efflux of Cmab through extracellular vesicles (EVs) [2]. In the case of colorectal cancer, mutations in *K-ras* and *B-raf*, downstream effectors of EGFR signaling, have been shown to predict Cmab resistance [34]. However, these mutations are very rare in HNSC. *PIK3CA* and *RAS* mutations and *PTEN* expression are potential biomarkers in HNSC [7,35]. The molecular mechanisms underlying Cmab resistance in HNSC were unknown before our current study. Our data clearly indicated that the difference in basal expression of EGFR between SAS and HSC-3 cells reflects the difference in the effect of Cmab (Fig. 2), which is consistent with the previous idea that the EGFR expression level is a predictive biomarker for the clinical efficacy of Cmab.

Our data also suggested that soluble EpEX stimulation promoted the proteolytic cleavage of cellular EpCAM, followed by the generation and nuclear translocation of EpICD. Both soluble EpEX and membrane-bound EpCAM are known to directly bind to EGFR via the EGF-like domain I and activate the EGFR signaling [19]. Since both soluble EpEX and cellular FL-EpCAM activate EGFR signaling, the signal may be transmitted in an autocrine or paracrine fashion [19]. Therefore, shedding the EpEX domain from cell-surface EpCAM may be a key mechanism to activate the EGFR signaling. Liang et al. showed that EpEX is a regulator of EpCAM shedding in HCT116 colon cancer cells and, more broadly speaking, regulates intramembrane proteolysis (RIP) [20]. Our data indicated that the generation and nuclear translocation of EpICD occurred after the soluble EpEX-dependent activation of the EGFR-ERK signaling pathway (Fig. 3, Fig. S3). Consistent with our present results, Hsu et al. showed that EpCAM cleavage in endometrial cancer cells is activated via the EGF/EGFR pathway [36]. Maetzel et al. first reported EpCAM functions as an intracellular signaling molecule [37]. EpCAM is degraded by a TNF-α converting enzyme (TACE, also known as a disintegrin and metallopeptidase domain 17 [ADAM17]) and presenilin 2, part of the γ-secretase complex, at the plasma membrane in the process of RIP [38]. This EpCAM cleavage is stimulated by soluble EpEX binding, cell-to-cell contact, and EGFR signaling [37–39]. Cleavage of EpCAM releases EpICD into first the cytoplasm and then the nucleus. Nuclear EpICD binds to FHL2, LEF1, and β-catenin to form a DNA binding complex that stimulates the transcription of target genes. This transcriptional regulation may be involved in the mechanism of Cmab resistance induced by EpCAM cleavage. Further investigation is required to clarify the key molecular mechanisms of EpCAM cleavage and the essential roles of EpICD in Cmab resistance.

Nuclear expression of EpICD has been reported to be an indicator of more aggressive tumor progression in HNSC [40], thyroid cancer [41], breast cancer [42], cholangiocarcinoma [43], and pancreatic adenocarcinoma [44]. A comprehensive study examining 10 epithelial carcinomas demonstrated that cytoplasmic and nuclear expression of EpICD is frequently observed in tumors but is not usually observed in normal tissue [45]. In some cancer types, membranous EpCAM expression is lost while cytoplasmic and nuclear expression increases. Our study indicated that nuclear translocation of ICD induced via EpEX and EGFR is a key mechanism of Cmab resistance and a promising biomarker of Cmab-resistance in HNC.

EpCAM is also involved in EVs, EMT, and cancer stem cells (CSC), associated with cancer drug resistance. EpCAM is expressed in CSCs and CSC-derived EVs in many cancer types [11,28,29,31,46–48]. Moreover,

the expression and release of EpCAM are associated with EMT and partial EMT [11,29]. EpEX is a ligand of EGFR that counteracts EGF-mediated EMT through modulation of phospho-ERK1/2 in HNC [18]. Nevertheless, it has been shown that EpEX enhances tumor progression through EGFR signaling in colon cancer cells [20]. In addition, EpEX signaling promotes tumor progression and protein stability of PD-L1 through the EGFR pathway [19]. And finally, EpEX and Oct4 are sufficient to generate iPS cells [49]. Thus, the EpEX-activated EGFR signaling, immune checkpoint, and stemness might be involved in the mechanism of drug resistance in cancer.

Conclusion

The soluble EpEX is an activating ligand for EGFR and a competitive antagonist against Cmab, by which HNSC cells lose their Cmab sensitivity and increase their Cmab resistance. The EpEX-activated Cmab resistance in HNSC could be mediated by the activation of the EGFR-ERK signaling pathway and the EpCAM cleavage-induced nuclear translocation of EpICD (Fig. 6). High expression and cleavage of EpCAM is thus a predictive biomarker for the clinical efficacy and resistance to Cmab.

Author contributions

KiO, TE, and SI conceptualized and designed the study. KiO, TE, HY, TOk, HN and SI prepared resources. KiO, TN, HoK, KyO, SR and TOk devised the methodologies. KU, TOg, KY, HiK and KS carried out the experimentation. HoK and NK performed formal analyses. KiO and KyO interpreted the data. KiO wrote the manuscript. KU, KiO and TE revised and edited the manuscript. All authors reviewed the manuscript.

Funding

This work was supported by Japan Society for Promotion of Science (JSPS) KAKENHI Grants-in-Aid for Scientific Research (19K24072 and 21K17115), the Wesco Scientific Promotion Foundation, and the KAWASAKI Foundation for Medical Science and Medical Welfare.

Declaration of Competing Interest

The authors declare that they have no known competing financial interests or personal relationships that could have appeared to influence the work reported in this paper.

Appendix A. Supplementary data

Supplementary data to this article can be found online at https://doi.org/10.1016/j.oraloncology.2023.106433.

References

[1] Fujiwara T, Eguchi T, Sogawa C, Ono K, Murakami J, Ibaragi S, et al. Carcinogenic epithelial-mesenchymal transition initiated by oral cancer exosomes is inhibited by anti-EGFR antibody cetuximab. Oral Oncol 2018;86:251–7.
[2] Fujiwara T, Eguchi T, Sogawa C, Ono K, Murakami J, Ibaragi S, et al. Anti-EGFR antibody cetuximab is secreted by oral squamous cell carcinoma and alters EGF-driven mesenchymal transition. Biochem Biophys Res Commun 2018;503:1267–72.
[3] Shimizu R, Ibaragi S, Eguchi T, Kuwajima D, Kodama S, Nishioka T, et al. Nicotine promotes lymph node metastasis and cetuximab resistance in head and neck squamous cell carcinoma. Int J Oncol 2019;54:283–94.
[4] Li S, Schmitz KR, Jeffrey PD, Wiltzius JJ, Kussie P, Ferguson KM. Structural basis for inhibition of the epidermal growth factor receptor by cetuximab. Cancer Cell 2005;7:301–11.
[5] Vermorken JB, Mesia R, Rivera F, Remenar E, Kawecki A, Rottey S, et al. Platinum-based chemotherapy plus cetuximab in head and neck cancer. N Engl J Med 2008;359:1116–27.
[6] Stanbouly D, Philipone E, Morlandt AB, Kaleem A, Chuang SK, Patel N. Adverse events secondary to cetuximab therapy in head & neck cancer therapy and risk factors for serious outcomes. Oral Oncol 2022;131:105952.
[7] Eze N, Lee JW, Yang DH, Zhu F, Neumeister V, Sandoval-Schaefer T, et al. PTEN loss is associated with resistance to cetuximab in patients with head and neck squamous cell carcinoma. Oral Oncol 2019;91:69–78.
[8] Piao HY, Qu JL, Liu YP. SOX8 promotes cetuximab resistance via HGF/MET bypass pathway activation in colorectal cancer. Cancer Chemother Pharmacol 2022;89:441–9.
[9] Yonesaka K, Zejnullahu K, Okamoto I, Satoh T, Cappuzzo F, Souglakos J, et al. Activation of ERBB2 signaling causes resistance to the EGFR-directed therapeutic antibody cetuximab. Sci Transl Med 2011;3:99ra86.
[10] Brand TM, Iida M, Wheeler DL. Molecular mechanisms of resistance to the EGFR monoclonal antibody cetuximab. Cancer Biol Ther 2011;11:777–92.
[11] Eguchi T, Sogawa C, Okusha Y, Uchibe K, Iinuma R, Ono K, et al. Organoids with cancer stem cell-like properties secrete exosomes and HSP90 in a 3D nanoenvironment. PLoS One 2018;13:e0191109.
[12] Gires O, Pan M, Schinke H, Canis M, Baeuerle PA. Expression and function of epithelial cell adhesion molecule EpCAM: where are we after 40 years? Cancer Metastasis Rev 2020;39:969–87.
[13] Brown TC, Sankpal NV, Gillanders WE. Functional Implications of the Dynamic Regulation of EpCAM during Epithelial-to-Mesenchymal Transition. Biomolecules 2021:11.
[14] Went PT, Lugli A, Meier S, Bundi M, Mirlacher M, Sauter G, et al. Frequent EpCam protein expression in human carcinomas. Hum Pathol 2004;35:122–8.
[15] Keller L, Werner S, Pantel K. Biology and clinical relevance of EpCAM. Cell Stress 2019;3:165–80.
[16] He HC, Kashat L, Kak I, Kunavisarut T, Gundelach R, Kim D, et al. An Ep-ICD based index is a marker of aggressiveness and poor prognosis in thyroid carcinoma. PLoS One 2012;7:e42893.
[17] Lin CW, Liao MY, Lin WW, Wang YP, Lu TY, Wu HC. Epithelial cell adhesion molecule regulates tumor initiation and tumorigenesis via activating reprogramming factors and epithelial-mesenchymal transition gene expression in colon cancer. J Biol Chem 2012;287:39449–59.
[18] Pan M, Schinke H, Luxenburger E, Kranz G, Shakhtour J, Libl D, et al. EpCAM ectodomain EpEX is a ligand of EGFR that counteracts EGF-mediated epithelial-mesenchymal transition through modulation of phospho-ERK1/2 in head and neck cancers. PLoS Biol 2018;16:e2006624.
[19] Chen HN, Liang KH, Lai JK, Lan CH, Liao MY, Hung SH, et al. EpCAM Signaling Promotes Tumor Progression and Protein Stability of PD-L1 through the EGFR Pathway. Cancer Res 2020;80:5035–50.
[20] Liang KH, Tso HC, Hung SH, Kuan II, Lai JK, Ke FY, et al. Extracellular domain of EpCAM enhances tumor progression through EGFR signaling in colon cancer cells. Cancer Lett 2018;433:165–75.
[21] Team RC. R: A language and environment for statistical computing. Vienna, Austria: R Foundation for Statistical Computing; 2022.
[22] Tang G, Cho M, Wang X. OncoDB: an interactive online database for analysis of gene expression and viral infection in cancer. Nucleic Acids Res 2022;50. D1334-D9.
[23] Lánczky A, Győrffy B. Web-Based Survival Analysis Tool Tailored for Medical Research (KMplot): Development and Implementation. J Med Internet Res 2021;23:e27633.
[24] Ono K, Eguchi T. Large-scale databases and portals on cancer genome to analyze chaperone genes correlated to patient prognosis. Methods Mol Biol 2023.
[25] Ono K, Sato K, Nakamura T, Yoshida Y, Murata S, Yoshida K, et al. Reproduction of the Antitumor Effect of Cisplatin and Cetuximab Using a Three-dimensional Spheroid Model in Oral Cancer. Int J Med Sci 2022;19:1320–33.
[26] Namba Y, Sogawa C, Okusha Y, Kawai H, Itagaki M, Ono K, et al. Depletion of Lipid Efflux Pump ABCG1 Triggers the Intracellular Accumulation of Extracellular Vesicles and Reduces Aggregation and Tumorigenesis of Metastatic Cancer Cells. Front Oncol 2018;8:376.
[27] Taha EA, Sogawa C, Okusha Y, Kawai H, Oo MW, Elseoudi A, et al. Knockout of MMP3 Weakens Solid Tumor Organoids and Cancer Extracellular Vesicles. Cancers (Basel) 2020:12.
[28] Sogawa C, Eguchi T, Namba Y, Okusha Y, Aoyama E, Ohyama K, et al. Gel-Free 3D Tumoroids with Stem Cell Properties Modeling Drug Resistance to Cisplatin and Imatinib in Metastatic Colorectal Cancer. Cells 2021:10.
[29] Ono K, Eguchi T, Sogawa C, Calderwood SK, Futagawa J, Kasai T, et al. HSP-enriched properties of extracellular vesicles involve survival of metastatic oral cancer cells. J Cell Biochem 2018;119:7350–62.
[30] Ono K, Okusha Y, Tran MT, Umemori K, Eguchi T. Western Blot Protocols for Analysis of CCN Proteins and Fragments in Exosomes, Vesicle-Free Fractions, and Cells. Methods Mol Biol 2023;2582:39–57.
[31] Ono K, Sogawa C, Kawai H, Tran MT, Taha EA, Lu Y, et al. Triple knockdown of CDC37, HSP90-alpha and HSP90-beta diminishes extracellular vesicles-driven malignancy events and macrophage M2 polarization in oral cancer. J Extracell Vesicles 2020;9:1769373.
[32] Sogawa C, Eguchi T, Okusha Y, Ono K, Ohyama K, Iizuka M, et al. A Reporter System Evaluates Tumorigenesis, Metastasis, β-catenin/MMP Regulation, and Druggability. Tissue Eng Part A 2019;25:1413–25.
[33] Thomas SM, Grandis JR. Pharmacokinetic and pharmacodynamic properties of EGFR inhibitors under clinical investigation. Cancer Treat Rev 2004;30:255–68.
[34] Karapetis CS, Jonker D, Daneshmand M, Hanson JE, O'Callaghan CJ, Marginean C, et al. PIK3CA, BRAF, and PTEN status and benefit from cetuximab in the treatment of advanced colorectal cancer–results from NCIC CTG/AGITG CO.17. Clin Cancer Res 2014;20:744–53.
[35] Leblanc O, Vacher S, Lecerf C, Jeannot E, Klijanienko J, Berger F, et al. Biomarkers of cetuximab resistance in patients with head and neck squamous cell carcinoma. Cancer Biol Med 2020;17:208–17.

[36] Hsu YT, Osmulski P, Wang Y, Huang YW, Liu L, Ruan J, et al. EpCAM-Regulated Transcription Exerts Influences on Nanomechanical Properties of Endometrial Cancer Cells That Promote Epithelial-to-Mesenchymal Transition. Cancer Res 2016;76:6171–82.
[37] Maetzel D, Denzel S, Mack B, Canis M, Went P, Benk M, et al. Nuclear signalling by tumour-associated antigen EpCAM. Nat Cell Biol 2009;11:162–71.
[38] Huang Y, Chanou A, Kranz G, Pan M, Kohlbauer V, Ettinger A, et al. Membrane-associated epithelial cell adhesion molecule is slowly cleaved by γ-secretase prior to efficient proteasomal degradation of its intracellular domain. J Biol Chem 2019; 294:3051–64.
[39] Nelson WJ, Nusse R. Convergence of Wnt, beta-catenin, and cadherin pathways. Science 2004;303:1483–7.
[40] Somasundaram RT, Kaur J, Leong I, MacMillan C, Witterick IJ, Walfish PG, et al. Subcellular differential expression of Ep-ICD in oral dysplasia and cancer is associated with disease progression and prognosis. BMC Cancer 2016;16:486.
[41] Kunavisarut T, Kak I, Macmillan C, Ralhan R, Walfish PG. Immunohistochemical analysis based Ep-ICD subcellular localization index (ESLI) is a novel marker for metastatic papillary thyroid microcarcinoma. BMC Cancer 2012;12:523.
[42] Srivastava G, Assi J, Kashat L, Matta A, Chang M, Walfish PG, et al. Nuclear Ep-ICD accumulation predicts aggressive clinical course in early stage breast cancer patients. BMC Cancer 2014;14:726.
[43] Jachin S, Bae JS, Sung JJ, Park HS, Jang KY, Chung MJ, et al. The role of nuclear EpICD in extrahepatic cholangiocarcinoma: association with β-catenin. Int J Oncol 2014;45:691–8.
[44] Fong D, Moser P, Kasal A, Seeber A, Gastl G, Martowicz A, et al. Loss of membranous expression of the intracellular domain of EpCAM is a frequent event and predicts poor survival in patients with pancreatic cancer. Histopathology 2014;64:683–92.
[45] Ralhan R, He HC, So AK, Tripathi SC, Kumar M, Hasan MR, et al. Nuclear and cytoplasmic accumulation of Ep-ICD is frequently detected in human epithelial cancers. PLoS One 2010;5:e14130.
[46] Fu C, Xiao X, Xu H, Lu W, Wang Y. Efficacy of atovaquone on EpCAM(+)CD44(+) HCT-116 human colon cancer stem cells under hypoxia. Exp Ther Med 2020;20: 286.
[47] Takai A, Fako V, Dang H, Forgues M, Yu Z, Budhu A, et al. Three-dimensional Organotypic Culture Models of Human Hepatocellular Carcinoma. Sci Rep 2016;6: 21174.
[48] Ruscetti M, Quach B, Dadashian EL, Mulholland DJ, Wu H. Tracking and Functional Characterization of Epithelial-Mesenchymal Transition and Mesenchymal Tumor Cells during Prostate Cancer Metastasis. Cancer Res 2015;75: 2749–59.
[49] Kuan II, Liang KH, Wang YP, Kuo TW, Meir YJ, Wu SC, et al. EpEX/EpCAM and Oct4 or Klf4 alone are sufficient to generate induced pluripotent stem cells through STAT3 and HIF2α. Sci Rep 2017;7:41852.